New Journal of Physics
The open-access journal for physics

# Double-negative acoustic metamaterials based on quasi-two-dimensional fluid-like shells

**Rogelio Graciá-Salgado, Daniel Torrent and José Sánchez-Dehesa**[1]

Wave Phenomena Group, Universitat Politècnica de València, Camino de Vera s.n. (Edificio 7F), E-46022 Valencia, Spain
E-mail: jsdehesa@upvnet.upv.es

*New Journal of Physics* **14** (2012) 103052 (15pp)
Received 12 July 2012
Published 31 October 2012
Online at http://www.njp.org/
doi:10.1088/1367-2630/14/10/103052

**Abstract.** A structured cylindrical scatterer with low-frequency resonances in both the effective bulk modulus and the dynamical mass density is designed and characterized. The proposed scattering unit is made of a rigid cylinder surrounded by a fluid-like shell embedded in a two-dimensional waveguide of height less than the length of the cylindrical scatterer. It is demonstrated that the acoustic metamaterials based on this building unit have negative acoustic parameters in a broad range of frequencies. It is also shown that double-negative behavior can be tailored by adjusting the dimensions and properties of the materials forming the structured scattering unit.

[1] Author to whom any correspondence should be addressed.

## Contents



## 1. Introduction

Acoustic metamaterials have become a topic of intensive research within the last few years [1]. These artificial structures are essentially periodic composites of sonic scatterers such that, for wavelengths larger than the periodicity of the building blocks, they behave like effective media with unusual acoustic parameters, such as anisotropic mass density [2–5], negative bulk modulus [6–8], negative mass density [9, 10] or both of them simultaneously [11–15]. There are many potential applications of these extraordinary materials, such as acoustic cloaking shells [16, 17], radial wave crystals [18, 19], subwavelength resonators [5], hyperlenses [20], gradient index lenses [21, 22], superlenses [23] and many other devices proposed within the framework of transformation-based solutions [24, 25].

For airborne propagation, it has been shown that anisotropic fluid-like metamaterials are relatively easy to fabricate [3–5]. Metamaterials with negative bulk modulus have also been experimentally characterized [6–8]. However, the fabrication of negative mass density metamaterials is not as simple, since negative mass is obtained by using complex structures, most of them containing membranes [9, 10, 26]. Consequently, structures exhibiting double-negative behavior are still scarce although the conditions for making them are relatively well established.

It was recently shown that an effective medium with negative mass density can be obtained using a cluster of scatterers or shells softer than the background [27], i.e. with both a mass density and a speed of sound smaller than that of the background. These properties are easy to obtain for an aqueous background, since many natural materials are acoustically soft when embedded in water. However, in the case of an air environment, where almost all the solid materials are acoustically rigid, the required properties are difficult to obtain and robust solutions are still needed.

The aim of this work is to demonstrate that metamaterials with negative mass or double-negative behavior for airborne sound propagation can be engineered by simple scatterers not involving membranes. On the one hand, the metamaterials proposed here make use of fluid-like metamaterials which have a speed of sound smaller than that in air but a larger effective mass. These properties are unusual for natural fluids but can be engineered at subwavelength frequencies by using lattices of rigid rods in air [28–30]. On the other hand, metamaterials with an effective mass density smaller than that of air can be obtained by considering the case of

sound propagation inside two-dimensional (2D) waveguides. Effectively, it has been shown that a step discontinuity or a cavity in a 2D waveguide behaves as a scatterer with a mass density smaller than that of the background. This effect has recently been used for the realization of anisotropic fluid-like metamaterials [3, 5].

The two effects mentioned above are combined in an acoustically soft scatterer consisting of a cavity drilled in a 2D waveguide where a rigid core is surrounded by a shell made of a cluster of small rigid cylinders. Note that this shell acts as a metamaterial with a sound speed smaller than air, while the cavity produces a dynamical density smaller than air. It is found that this complex scatterer can be used as a building block for realization of double-negative acoustic metamaterials for airborne propagation.

This paper is organized as follows. In section 2 the scattering unit is studied in the low-frequency limit and the effective parameters are obtained by solving the scattering problem of an isolated unit embedded in a 2D waveguide. Although the scattering problem is strictly three dimensional, we name it 'quasi-2D' because we only consider waves with wavevectors contained in the $XY$-plane. In spite of this, the third direction (the $z$-axis) is taken into account since the unit penetrates one of the surfaces defining the waveguide. Afterwards, in section 3, the problem for a lattice of scattering units is solved. Also, the effective parameters of the resulting quasi-2D metamaterial are studied as a function of the geometrical dimensions of the structured units in order to find the dimensions where both the bulk modulus and the density are simultaneously negative. Finally, the results are summarized in section 4. The appendix describes the procedure to obtain the $T$ matrix of the structured unit proposed here.

## 2. Effective parameters of the structured scatterer: $B_a(\omega)$ and $\rho_a(\omega)$

The structures under study are schematically depicted in figure 1(a). They consist of arrays of cylindrical scatterers embedded in a 2D waveguide with height $h$ and the cylinders penetrate a length $L$ into the upper surface of the waveguide. Each individual scatterer has an inner structure that is described in figure 1(b). Each scatterer is made by drilling a cylindrical cavity of radius $R_b$ and depth $L$ in one of the two acoustically rigid surfaces defining a 2D waveguide. The cavity is then filled with a rigid cylinder of radius $R_a < R_b$ and surrounded by a fluid-like shell that must have a mass density $\rho_s > \rho_b$ and sound speed $c_s < c_b$, where $\rho_b$ and $c_b$ are the static mass density and speed of sound, respectively, of the background (air in this work). It is interesting to stress that there are six parameters that can be adjusted in order to tailor the acoustic properties of the designed unit: $R_a$, $R_b$, $L$, $h$, $c_s$ and $\rho_b$.

The wavelength inside the proposed shell is shorter than that of the background since $c_s < c_b$. Then, although outside the scatterer the sound wavelength can be much larger than $R_a$, the pressure field inside the shell can exhibit oscillatory behavior, leading to a set of resonances responsible for the metamaterial behavior, as has already been discussed in [27, 31].

If the cavity in figure 1 does not exist (i.e. $L = 0$) the effective density of the structured unit is larger than that of the background, but can be made smaller just using $L > 0$ as explained below.

The possibility of engineering mass densities smaller than that of air has been proved in [3, 5], where it was shown that a hole with depth $L$ in a 2D air waveguide behaves like a sound scatterer with an equal speed of sound and mass density given by $\rho_{hole} \approx h/(h+L)\rho_0$, $h$ being the height of the waveguide and $L$ the hole depth. So, if the cavity is filled with a fluid of density $\rho_s$ and a speed of sound $c_s$, the full system will behave as a scatterer with mass density

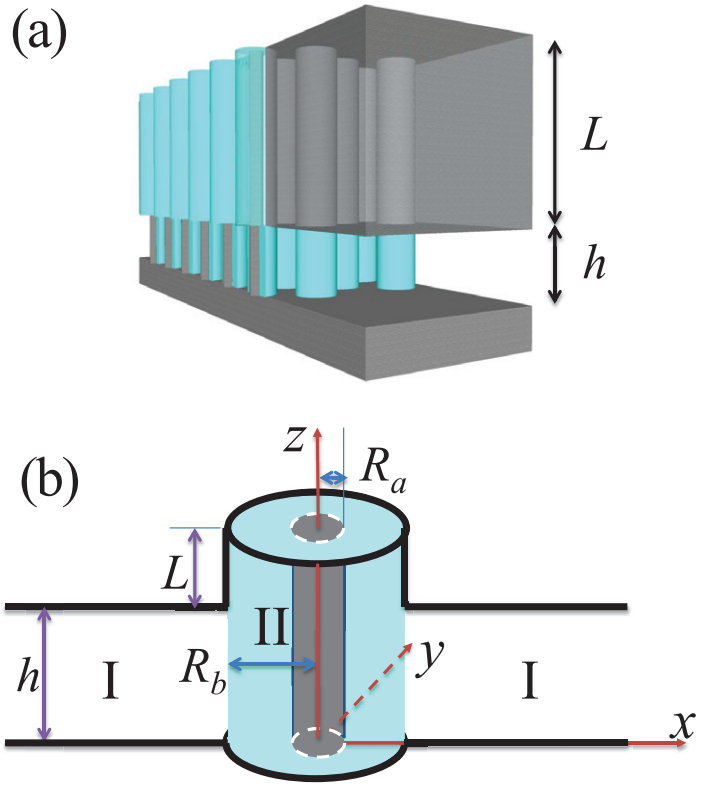


**Figure 1.** (a) Schematic view of the structures under study. They consist of an array of cylindrical scatterers embedded in a 2D waveguide. Note that the scatterer units penetrate the upper part of the waveguide. (b) Scheme of an individual scatterer. It is made of a cylindrical cavity of length $L$ and radius $R_b$ that is drilled into the 2D waveguide with height $h$ (region I). An acoustically rigid cylinder of radius $R_a$ (black cylinder) with length $L+h$ is placed at the center of the cavity and is surrounded by a fluid-like shell (region II) with dynamical mass density $\rho_s > \rho_b$ and effective speed of sound $c_s < c_b$, where $\rho_b$ and $c_b$ are the static density and the phase velocity, respectively, of the background fluid in region I.

given by

$$\rho_a \approx \frac{h}{h+L}\rho_s. \tag{1}$$

This expression indicates that increasing $L$ reduces the effective density of the fluid, obtaining then a sound scatterer for airborne propagation in which both the speed of sound and the density are smaller than those of the background. Therefore, this structure is a good candidate for showing double-negative parameters. This model for the effective density of the proposed scatterer unit is only qualitative and should be supported with better predictions involving the solution of the complete scattering problem as is shown below.

In the framework of multiple scattering theory, the $T$ matrix has a complex magnitude that is frequency dependent and relates the scattered field by the sonic scatterer to the incident acoustic field. It was shown in [27] that for the case of a cylindrical scatterer with subwavelength

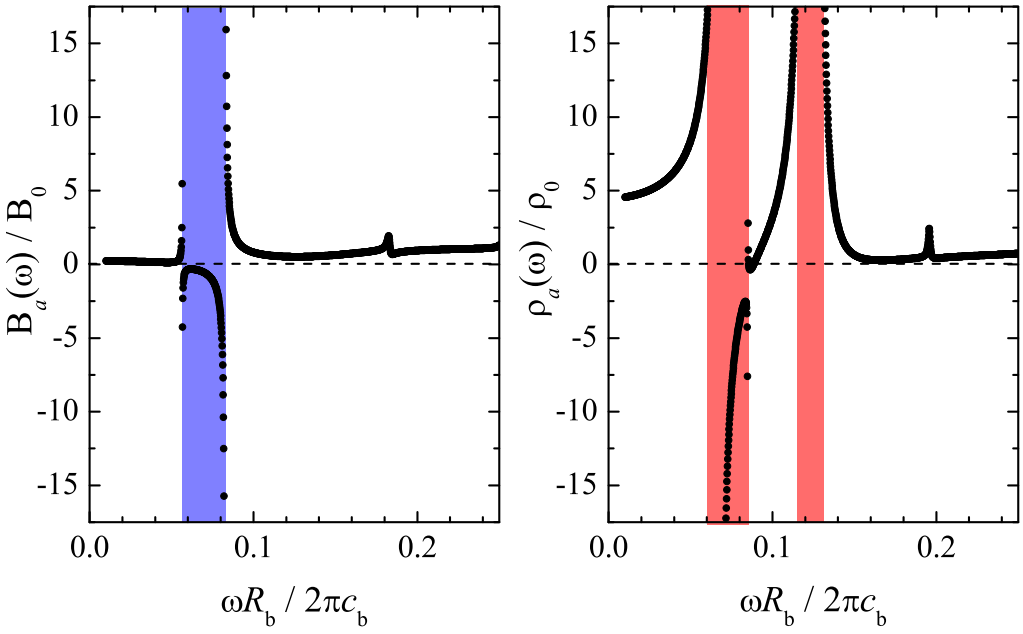


**Figure 2.** Frequency dependence (in reduced units) of the effective bulk modulus (left panel) and the dynamical mass density (right panel) of the shell depicted in figure 1 with parameters $h = R_b$, $L = R_b$, $R_a = 0,5R_b$, $\rho_s = 4\rho_b$ and $c_s = 0.3c_b$. The colored bands define the frequencies with negative values.

dimension, this matrix allows derivation of the frequency-dependent bulk modulus $B_a$ and mass density $\rho_a$, which take the following expressions:

$$B_a(\omega)/B_b = \frac{k_b^2 R_b^2}{2} \ln k_b R_b - \frac{1}{2} k_b R_b \chi_0, \tag{2a}$$

$$\rho_a(\omega)/\rho_b = \frac{\chi_1}{k_b R_b}, \tag{2b}$$

where $B_b$ and $\rho_b$ are the parameters of the background, $k_b = \omega/c_b$ is the background's wavenumber and $R_b$ is the scatterer's external radius. Finally, $\chi_0$ and $\chi_1$ are quantities whose explicit expressions are obtained from the $T$ matrix and are displayed in the appendix.

The typical behavior of the effective parameters $B_a(\omega)$ and $\rho_a(\omega)$ is depicted in figure 2 for the scattering unit depicted in figure 1 with $L = h = R_b$, $\rho_s = 4\rho_b$ and $c_s = 0.3c_b$. Note how the parameters, which are given in normalized units, exhibit a complex frequency response due to the fact that inside the fluid-like shell (region II) the pressure field oscillates and, consequently, resonant processes take place. For example, figure 3(a) shows the pressure pattern calculated at the equatorial plane of the waveguide for the frequency 0.06 (in reduced units), where the bulk modulus is negative. This field represents a monopolar resonance that is responsible for the negative value [11]. On the other hand, figure 3(b) represents the pressure pattern calculated at the frequency 0.12, where the density takes a negative value. In this case the field pattern has the shape of a dipolar resonance, which explains the negative value of the effective density [11].

If these scattering units are employed as building blocks of lattices with subwavelength separation, the resulting effective medium will present negative acoustic parameters and, therefore, it represents a type of quasi-2D acoustic metamaterial. The metamaterial is called

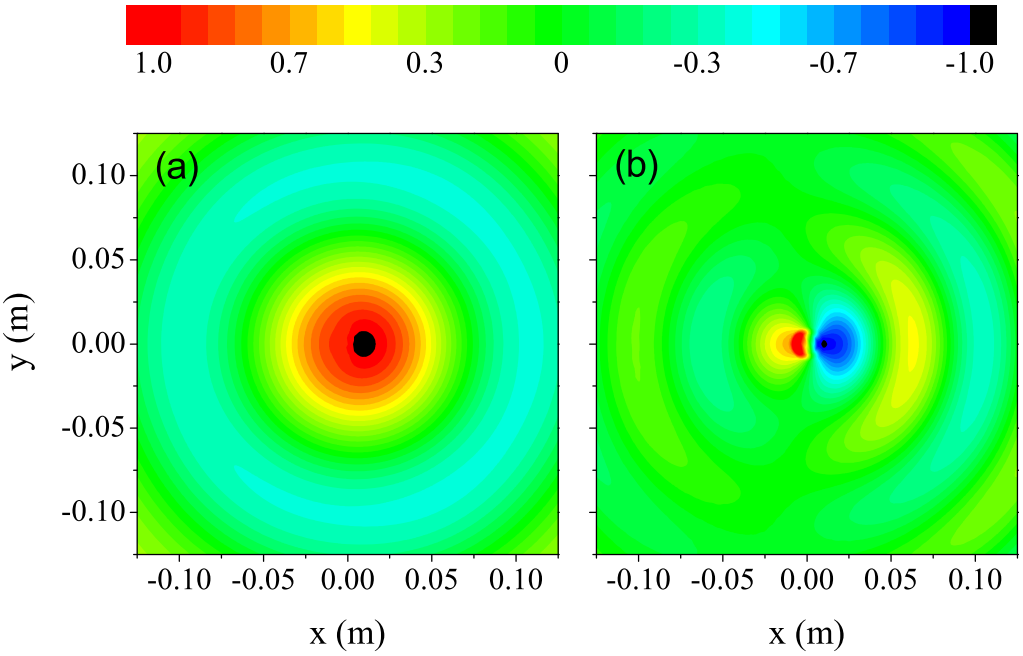


**Figure 3.** (a) Pressure map calculated at the frequency 0.06 (in reduced units) giving a negative value of the bulk modulus (see the left panel in figure 2). (b) Pressure map calculated at the frequency 0.12 (in reduced units) giving a negative dynamical mass density (see the right panel in figure 2). The opening of the cavity is centered at (0, 0) and has a radius of 1 cm.

quasi-2D because its building unit contains a cavity of length $L$ drilled in one of the boundary surfaces defining the 2D waveguide. The parameters depend on the different dimensions of the structured unit ($R_b$, $R_a$, $h$ and $L$) as well as the material parameters of the shell ($\rho_s$, $c_s$). Analytical expressions of metamaterial parameters are not easy to obtain, but the next section shows that the results can be depicted in phase diagram plots where the conditions in which negative values appear are clearly shown.

## 3. Effective parameters of the acoustic metamaterial: $B^*(\omega)$ and $\rho^*(\omega)$

The effective parameters $B_a(\omega)$ and $\rho_a(\omega)$ of the structured unit studied above are employed here to derive the effective parameters for the metamaterials based on lattices using this unit as the building block.

Let us consider a 2D isotropic lattice (i.e. a hexagonal or square lattice) in which the fraction of volume occupied by the cylinders is $f$. Following the procedure described in [27], the effective parameters can be derived using the following expressions:

$$\frac{1}{B^*(\omega)} = \frac{1-f}{B_b} + \frac{f}{B_a(\omega)}, \tag{3a}$$

$$\rho^*(\omega) = \frac{(1+f)\rho_b + (1-f)\rho_a(\omega)}{(1-f)\rho_b + (1+f)\rho_a(\omega)}, \tag{3b}$$

where the terms of multiple scattering have not been included since we will consider metamaterials based on isotropic lattices with low $f$. More complicated arrangements, such as non-isotropic lattices and large $f$, can also be studied but these effects are beyond the scope of this work. For a detailed discussion of these effects on the acoustic parameters, see [27].

The resonances within the cavity shell generate effective acoustic parameters showing a strong oscillation passing through zero, between very negative values and very positive values. In this work, we are interested only in regions where the parameters change sign, since the sign defines the propagation regime in the metamaterial (see figure 3 in [27]). Note that the propagation is controlled by the phase velocity, which is given by

$$c^*(\omega) = \pm\sqrt{\frac{B^*(\omega)}{\rho^*(\omega)}}. \tag{4}$$

For example, when both the parameters, $B^*(\omega)$ and $\rho^*(\omega)$, are simultaneously positive or negative, the speed of sound is positive, or negative, respectively. However, when just one parameter is negative and the other is positive the resulting effective sound speed is purely imaginary, i.e. evanescent, and there is no propagation.

To study the sign of the effective parameters, we present the results in phase diagram plots, where the changes in sign of the effective parameters are deployed as a function of the frequency and a selected physical dimension of the structured scatterer (see figure 1). This form of data representation is especially useful when the magnitudes of interest depend on many parameters. See [30, 32] showing examples of how phase diagrams are already employed in acoustics to characterize magnitudes depending on several parameters.

In particular, we report two examples of phase diagrams: one in which $R_b$ and $R_a$ are kept constant, and we look for changes in sign as a function of the ratio $L/h$; and another in which this ratio is fixed and we look for changes in sign as a function of $R_a/R_b$. In both examples the waveguide height is set to $h = 0.44a$, where $a$ is the lattice constant of the hexagonal array in which the metamaterial units are distributed. This small value of $h$ is necessary in order to enhance the scattering effects of the fluid-like shell, and reinforces the quasi-2D nature of the system analyzed. Also, the external radius of the cavity is the same in the two cases, being $R_b = 0.44a = h$. This value of $R_b$ is chosen so that $f$ is large enough to observe scattering effects, but small enough to neglect the multiple scattering correction to the effective parameters.

In the two examples the cavity shell is filled with a fluid-like material of acoustic mass density $c_s = 0.3c_b$ and $\rho_s = 4\rho_b$. These values are not chosen at random; they correspond to the effective parameters that can be achieved by considering subwavelength arrangements of cylindrical scatterers [28, 29, 32, 33]. Thus, it can be said that the fluid-like shell is, in fact, an acoustic metafluid that can be engineered using a cluster of small cylindrical rods.

### *3.1. Phase diagrams in the plane $\omega$–$L/h$*

Figure 4 shows the phase diagrams for the effective bulk modulus (left panel) and density (right panel) for the case when the radius of the central rigid cylinder is $R_a = 0.5R_b$. The sweep is made in the $L/h$ ratio and the colored regions represent the values at which acoustic parameters have negative signs.

The left panel of figure 4 demonstrates that negative bulk modulus can be obtained above the cutoff value $L/h \gtrsim 0.5$, since above this cutoff the cavity acts as a Helmholtz resonator [8].

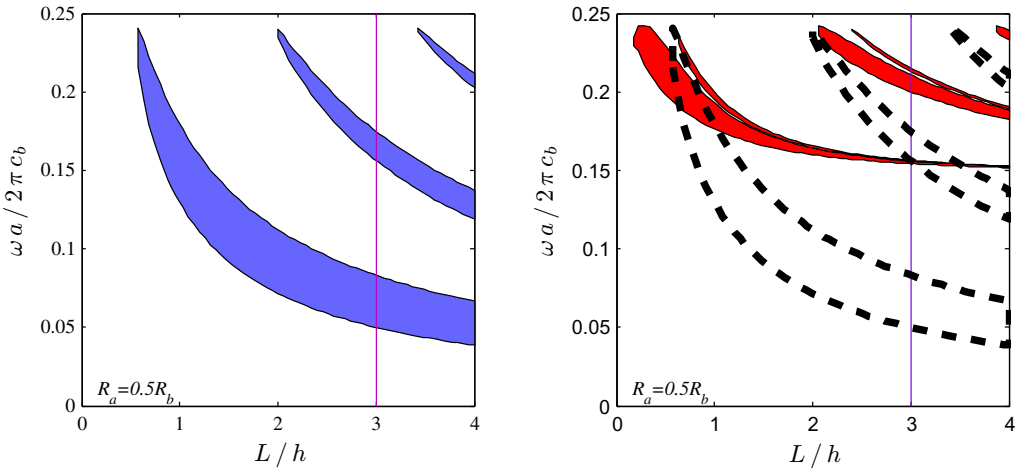


**Figure 4.** Colored regions give the values $\omega$–$L/h$ where the effective bulk modulus (left panel) and the effective mass density (right panel) are negative. Dashed lines enclose the regions with negative bulk modulus for comparison purposes; the overlaps with the negative mass density regions define the conditions where both parameters are negative simultaneously.

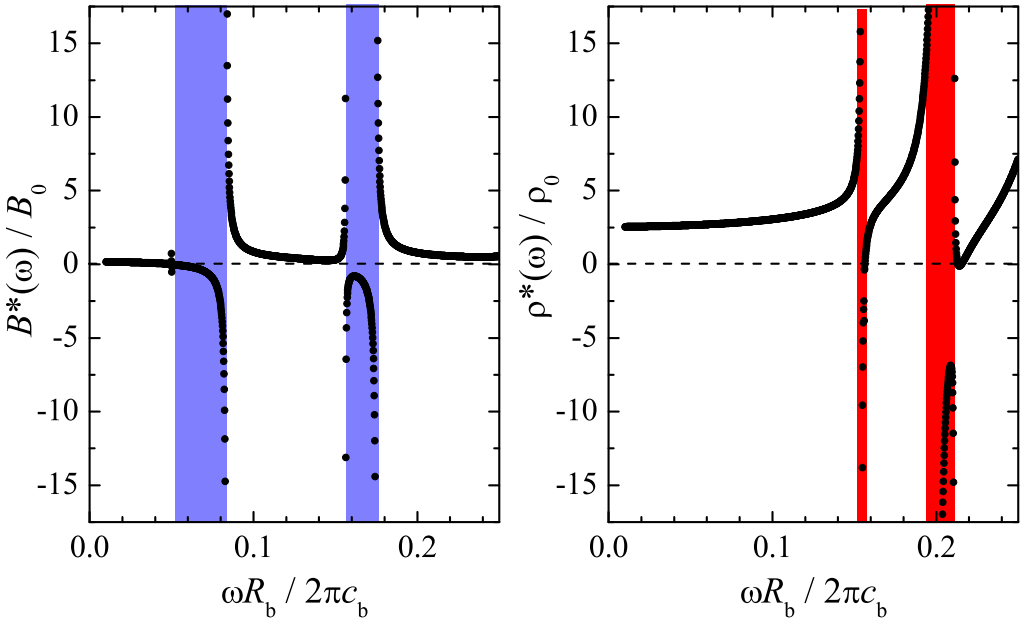


**Figure 5.** Effective bulk modulus (left panel) and effective mass density (right panel) as a function of the frequency for the structure analyzed in figure 4. These results correspond to a cut through the line $L = 3h$ in the phase diagram seen in figure 4. The horizontal dashed lines define the level zero of the corresponding acoustic parameter.

It is also observed that the frequency band at which this negative sign appears gets smaller as we increase the length $L$, and additional bands with negative modulus appear. This is due to the resonances of the cavity, whose number increases as we extend its length, acting as a tube [8].

The right panel of figure 4 shows that the negative mass density also appears above a certain cutoff value of $L/h$, which is smaller now. The negative behavior is due to the fact that the cavity is filled with a metafluid with phase velocity $c_s = 0.3c_b$, which in principle would be enough to present negative mass density by itself. However, the coupling between the shell cavity and the outside sound is not efficient since the mass density of the fluid shell is $\rho_s = 4\rho_b$, which is too high. The coupling is possible because the effect of $L$ is to decrease the apparent mass density of the metafluid without changing the speed of sound. So, for small values of $L/h$ we quickly have an efficient coupling and therefore a negative effective mass density. In comparison with the case of effective modulus, it can be observed that now the regions with negative values are narrower in frequency. However, as we increase the depth $L$, more resonances appear and more regions of negative inertia are evolving as in the case of the effective modulus.

The right panel of figure 4 also shows a dashed line that encloses the region with negative bulk modulus depicted in the right panel. The overlap with the red regions defines the conditions in which we expect double-negative behavior, which is easily determined from these phase diagram plots. Note that a relatively broad frequency region with double-negative parameters should be obtained by using cavities with $0.63 \leqslant L/h \leqslant 1.03$. Double-negative parameters within a narrow frequency region should be obtained by using $3.00 \leqslant L/h \leqslant 3.50$.

Figure 5 shows the frequency-dependent effective bulk modulus (left panel) and mass density (right panel) extracted from figure 4 at $L/h = 3$, which is defined by the vertical red line in the phase diagram. We see that the effective parameters present regions of negativity according to the calculated phase diagram.

### *3.2. Phase diagrams in the plane $\omega$–$R_a/R_b$*

Figure 6 shows the phase diagrams for the effective bulk modulus (left panel) and density (right panel) for the same metamaterial studied in figure 4 but now the length is fixed at $L = h$, and the sweeping is done in the ratio $R_a/R_b$. Now the effective medium is more stable, since the number of resonances is only one and does not increase (note that this number is essentially a function of $L$). We can observe that as the ratio $R_a/R_b \to 1$, which means that the structured scatterer is becoming just a rigid cylinder, the negative behavior of the effective medium disappears, as is expected. We can also see that, although the frequency region of negative modulus varies slowly as a function of $R_a/R_b$, the region of negative density appears at a lower frequency for $R_a/R_b \approx 0.7$. This should be the appropriate working region since the lower the frequency where the metamaterial behavior appears, the better the effective medium approximation works. The overlap between the region with negative modulus (which is represented by the dashed line in the right panel) and that with negative density is obtained for values $0.45 \leqslant R_a/R_b \leqslant 0.88$, which should be used to construct the sample exhibiting negative refraction.

Figure 7 shows the effective parameters for the system described in figure 6 but at $R_a = 0.7R_b$, showing perfect agreement between the region of negative behavior for the bulk modulus and the mass density. In both plots some sharp resonances are observed at the reduced frequency of 0.134 (in the left panel) and at 0.218, 0.226 and a few more above (in the right panel). These peaks correspond to resonances of higher order that appear in the computation of the $T$ matrix, but they are too sharp to be observed in actual structures due to dissipation.

It is important to remark that more phase diagrams can be generated by changing the acoustic parameters (mass density and modulus) of the shell, as well as its filling fraction, radius

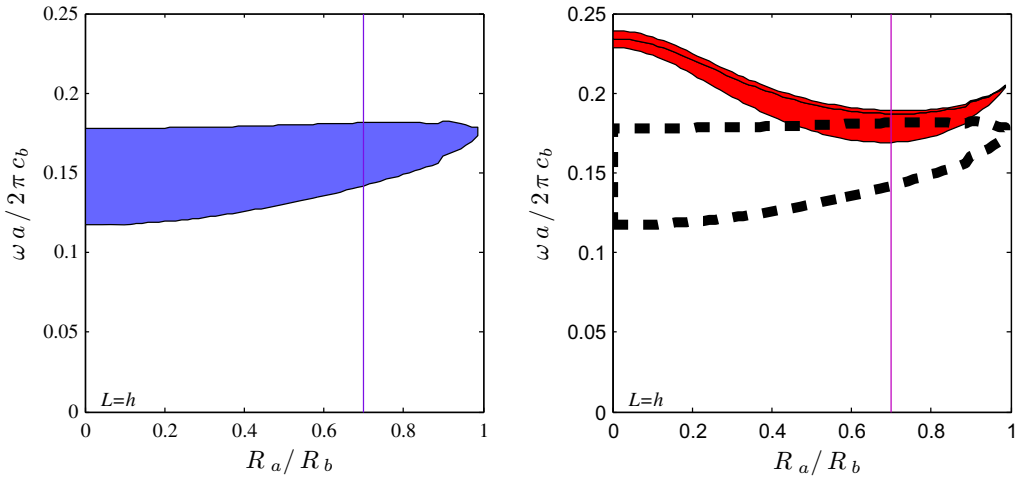


**Figure 6.** Colored regions define the values $\omega$–$R_a/R_b$ where the effective bulk modulus (blue region in the left panel) and the effective mass density (green region in the right panel) are negative. Dashed lines in the right panel enclose the region with negative bulk modulus for comparison purposes; the overlapping regions define the conditions in which double-negative parameters are expected.

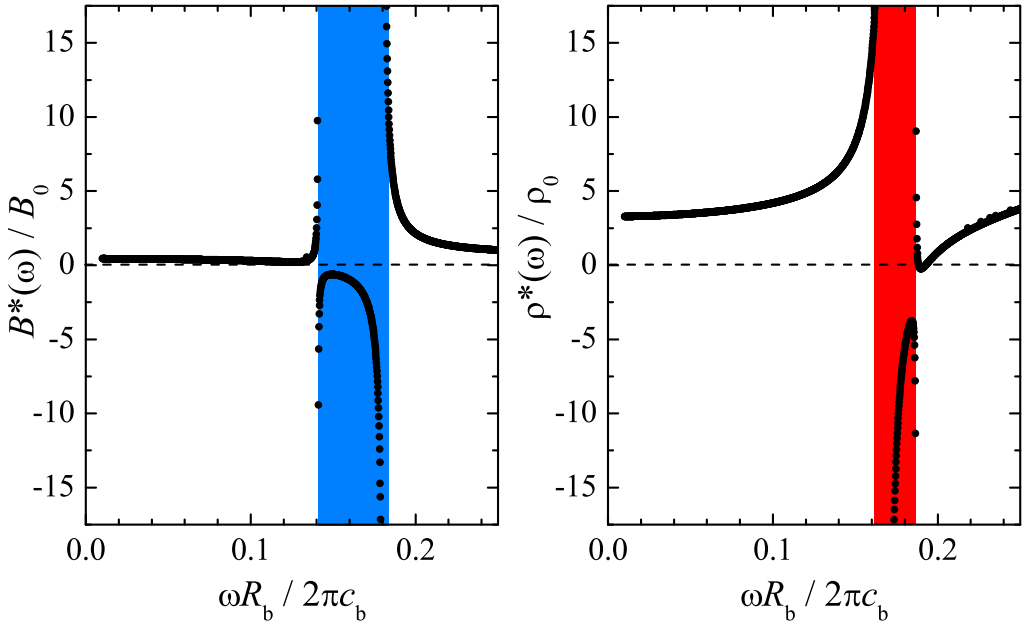


**Figure 7.** Frequency dependence of the effective bulk modulus (left panel) and dynamical mass density (right panel) for the structure studied in figure 6. These results correspond to a cut of the phase diagram along the line $R_a = 0.7R_b$. The horizontal dashed lines are a guide to the eyes, indicating the value zero for the corresponding acoustic parameter.

of the rigid cylinder, height of the cavity, etc. The degrees of freedom of this apparently simple scattering unit make it possible to design many types of 2D acoustic metamaterials. However, at the same time, this large number of degrees of freedom is the reason why these structures are

difficult to study. At any rate, we have shown that using this phase-diagram representation is a useful tool for determining the physical dimensions required to obtain the desired behavior.

## 4. Summary

In summary, we have introduced a new type of scattering unit for airborne sound propagating in a 2D waveguide that can be used for the design of either single- or double-negative acoustic metamaterials. The scatterer consists of a cavity drilled in a waveguide with a rigid cylinder inside it, with the rest of the cavity filled with a fluid-like material having a phase velocity smaller than air. This structured scatterer is especially suitable for designing acoustic metamaterials with negative parameters for airborne sound, but it can also be used as a building block feasible for underwater acoustics.

It has been reported that acoustic parameters can be tailored with a large number of degrees of freedom, such as the filling fraction, waveguide's height, cavity depth, etc, which makes the problem difficult to analyze. To overcome this difficulty, the results have been displayed in phase-diagram plots, which have become an extremely helpful tool for the design of negative metamaterials based on building units with many variables.

Although the practical realization of single- or double-negative acoustic metamaterials with low losses is challenging for airborne sound, the structured scattering unit proposed here is a good candidate for achieving that goal. We expect that the work presented here will motivate further experimental research supporting its predictions either for airborne sound or for underwater acoustics using similar units.

## Acknowledgments

This work was partially supported by the Spanish Ministerio de Ciencia e Innovacion (MICINN) under contracts TEC2010-19751 and CSD2008-66 (the CONSOLIDER program) and by the US Office of Naval Research. The authors acknowledge Victor M García-Chocano for useful discussions and Kimee Moore for proofreading the paper.

## Appendix. The $T$ matrix of a cylindrical scatterer consisting of a fluid shell surrounding a central rigid cylinder

This appendix is devoted to solving the scattering problem defined by the scattering unit depicted schematically in figure 1.

The pressure field in region I, which corresponds to the air surrounding the cylindrical scatterer (i.e. $r \geqslant R_b$), can be expanded as a linear combination of the solutions for the empty cavity, $\Phi_n^I(z)$, as follows:

$$P^I(r,\theta,z;\omega) = \sum_{n=0}^{\infty}\sum_{q=-\infty}^{\infty}\left[A_{qn}J_q(k_n^I r) + B_{qn}H_q(k_n^I r)\right]e^{iq\theta}\Phi_n^I(z), \tag{A.1}$$

where the coefficients $A_{qn}$ and $B_{qn}$ represent the incident and scattered fields, respectively. On the other hand, $\Phi_n^I(z)$ are normalized functions accomplishing the condition that the normal

velocity is zero at the bottom and upper surface walls, i.e. $\frac{\partial \Phi_n^{\mathrm{I}}(z)}{\partial z} = 0,\ \infty$ at $z = 0$ and $h$, respectively. In other words,

$$\Phi_n^{\mathrm{I}}(z) = \sqrt{\frac{\epsilon_n}{h}} \cos\left(\frac{n\pi}{h} z\right), \quad \epsilon_n = \begin{cases} 1 & \text{if } n = 0, \\ 2 & \text{if } n \neq 0. \end{cases} \tag{A.2}$$

Finally, $k_n^{\mathrm{I}}$ in equation (A.1) is the transverse wavenumber given by

$$k_n^{\mathrm{I}} = \sqrt{\left(\frac{\omega}{c_{\mathrm{b}}}\right)^2 - \left(\frac{n\pi}{h}\right)^2}, \tag{A.3}$$

where $n$ is an integer that can take values $n = 0, 1, \ldots, \infty$. We are interested here in the single-mode propagation regime, i.e. when $k_n^{\mathrm{I}}$ has only a real part and therefore $n = 0$. Note that $k_n^{\mathrm{I}}$ with only an imaginary part corresponds to evanescent solutions, which do not propagate through the waveguide but that must be considered for the efficient computation of the scattering coefficients.

For region II, where $R_{\mathrm{a}} \leqslant r \leqslant R_{\mathrm{b}}$, the field inside the fluid shell can be expanded as

$$P^{\mathrm{II}}(r, \theta, z) = \sum_{m=0}^{\infty} \sum_{q=-\infty}^{\infty} C_{qm} \left[ J_q(k_m^{\mathrm{II}} r) - \frac{\dot{J}_q(k_m^{\mathrm{II}} R_{\mathrm{a}})}{\dot{Y}_q(k_m^{\mathrm{II}} R_{\mathrm{a}})} Y_q(k_m^{\mathrm{II}} r) \right] \mathrm{e}^{\mathrm{i}q\theta} \Phi_m^{\mathrm{II}}(z), \tag{A.4}$$

where the normalized functions $\Phi_m^{\mathrm{II}}(z)$ are now

$$\Phi_m^{\mathrm{II}}(z) = \sqrt{\frac{\epsilon_m}{h + L}} \cos\left(\frac{m\pi}{h + L} z\right), \tag{A.5}$$

which satisfies the boundary condition $\partial P^{\mathrm{II}}/\partial r = 0$ at $z = 0, h + L$. The function $P^{\mathrm{II}}$ also verified the boundary condition at the surface of the rigid cylinder $r = R_{\mathrm{a}}$.

The transverse wavenumber is now

$$k_m^{\mathrm{II}} = \sqrt{\left(\frac{\omega}{c_{\mathrm{s}}}\right)^2 - \left(\frac{m\pi}{h + L}\right)^2}, \quad m = 0, 1, \ldots, \infty. \tag{A.6}$$

Now, we impose the continuity conditions of fields $P^{\mathrm{I}}$ $P^{\mathrm{II}}$ at the surface $r = R_{\mathrm{b}}$. The pressure continuity is obtained by projecting first on the waveguide modes and afterwards integrating from $z = 0$ to $h$:

$$\int_0^h P^{\mathrm{I}}(r, \theta, z)|_{r=R_{\mathrm{b}}} \Phi_k^{\mathrm{I}}(z)\, \mathrm{d}z = \int_0^h P^{\mathrm{II}}(r, \theta, z)|_{r=R_{\mathrm{b}}} \Phi_k^{\mathrm{I}}(z)\, \mathrm{d}z. \tag{A.7}$$

For the continuity of the normal component of the particle velocity, we project with the modes in the cavity and integrate from $z = 0$ to $h + L$, leading to

$$\frac{1}{\rho_{\mathrm{b}}} \int_0^{h+L} \left.\frac{\partial P^{\mathrm{I}}(r, \theta, z)}{\partial r}\right|_{r=R_{\mathrm{b}}} \Phi_k^{\mathrm{II}}(z)\, \mathrm{d}z = \frac{1}{\rho_{\mathrm{s}}} \int_0^{h+L} \left.\frac{\partial P^{\mathrm{II}}(r, \theta, z)}{\partial r}\right|_{r=R_{\mathrm{b}}} \Phi_k^{\mathrm{II}}(z)\, \mathrm{d}z. \tag{A.8}$$

After integrating the fields and using the orthogonality properties of the angular functions, equations (A.7) and (A.8) become, respectively,

$$A_{qk} J_q(k_k^{\mathrm{I}} R_{\mathrm{b}}) + B_{qk} H_q(k_k^{\mathrm{I}} R_{\mathrm{b}}) = \sum_{m=0}^{\infty} C_{qm} \left[ J_q(k_m^{\mathrm{II}} R_{\mathrm{b}}) - \frac{\dot{J}_q(k_m^{\mathrm{II}} R_{\mathrm{a}})}{\dot{Y}_q(k_m^{\mathrm{II}} R_{\mathrm{a}})} Y_q(k_m^{\mathrm{II}} R_{\mathrm{b}}) \right] G_{km} \tag{A.9}$$

and

$$\frac{1}{\rho_b}\sum_{n=0}^{\infty}\left[A_{qn}\dot{J}_q(k_n^{\mathrm{I}}R_b)+B_{qn}\dot{H}_q(k_n^{\mathrm{I}}R_b)\right]G_{nk}=\frac{1}{\rho_s}C_{qk}\left[\dot{J}_q(k_k^{\mathrm{II}}R_b)-\frac{\dot{J}_q(k_k^{\mathrm{II}}R_a)}{\dot{Y}_q(k_k^{\mathrm{II}}R_a)}\dot{Y}_q(k_k^{\mathrm{II}}R_b)\right]. \tag{A.10}$$

The coefficients $C_{qk}$ obtained from equation (A.10) as follows:

$$C_{qk}=\frac{\rho_s}{\rho_b}\sum_{n=0}^{\infty}\left[\frac{\dot{J}_q(k_n^{\mathrm{I}}R_b)G_{nk}}{\left[\dot{J}_q(k_k^{\mathrm{II}}R_b)-\frac{\dot{J}_q(k_k^{\mathrm{II}}R_a)}{\dot{Y}_q(k_k^{\mathrm{II}}R_a)}\dot{Y}_q(k_k^{\mathrm{II}}R_b)\right]}A_{qn}+\frac{\dot{H}_q(k_n^{\mathrm{I}}R_b)G_{nk}}{\left[\dot{J}_q(k_k^{\mathrm{II}}R_b)-\frac{\dot{J}_q(k_k^{\mathrm{II}}R_a)}{\dot{Y}_q(k_k^{\mathrm{II}}R_a)}\dot{Y}_q(k_k^{\mathrm{II}}R_b)\right]}B_{qn}\right] \tag{A.11}$$

and are inserted into equation (A.9) to obtain, after some tedious algebra, the following relation:

$$\begin{aligned}A_{qk}J_q(k_k^{\mathrm{I}}R_b)-\sum_{m=0}^{\infty}\frac{\rho_s}{\rho_b}\sum_{n=0}^{\infty}&\left[\frac{\dot{J}_q(k_n^{\mathrm{I}}R_b)J_q(k_m^{\mathrm{II}}R_b)G_{km}G_{nm}}{\left[\dot{J}_q(k_m^{\mathrm{II}}R_b)-\frac{\dot{J}_q(k_m^{\mathrm{II}}R_a)}{\dot{Y}_q(k_m^{\mathrm{II}}R_a)}\dot{Y}_q(k_m^{\mathrm{II}}R_b)\right]}A_{qn}\right.\\&\left.=-[B_{qk}H_q(k_k^{\mathrm{I}}R_b)-\sum_{m=0}^{\infty}\frac{\rho_s}{\rho_b}\sum_{n=0}^{\infty}\left[\frac{\dot{H}_q(k_n^{\mathrm{I}}R_b)J_q(k_m^{\mathrm{II}}R_b)G_{km}G_{nm}}{\left[\dot{J}_q(k_m^{\mathrm{II}}R_b)-\frac{\dot{J}_q(k_m^{\mathrm{II}}R_a)}{\dot{Y}_q(k_m^{\mathrm{II}}R_a)}\dot{Y}_q(k_m^{\mathrm{II}}R_b)\right]}B_{qn}\right].\end{aligned} \tag{A.12}$$

This equation can be cast in matrix form as

$$\sum_m(H_q)_{km}B_{qm}=\sum_n(J_q)_{kn}A_{qn} \tag{A.13}$$

with

$$(J_q)_{kn}\equiv J_q(k_n^{\mathrm{I}}R_b)\delta_{kn}-\frac{\rho_s}{\rho_b}\sum_m\frac{\dot{J}_q(k_n^{\mathrm{I}}R_b)G_{km}G_{nm}J_q(k_m^{\mathrm{II}}R_b)}{\dot{J}_q(k_m^{\mathrm{II}}R_b)-\frac{\dot{J}_q(k_m^{\mathrm{II}}R_a)}{\dot{Y}_q(k_m^{\mathrm{II}}R_a)}\dot{Y}_q(k_m^{\mathrm{II}}R_b)}, \tag{A.14}$$

$$(H_q)_{kn}\equiv-\left[H_q(k_n^{\mathrm{I}}R_b)\delta_{kn}-\frac{\rho_s}{\rho_b}\sum_m\frac{\dot{H}_q(k_n^{\mathrm{I}}R_b)G_{km}G_{nm}J_q(k_m^{\mathrm{II}}R_b)}{\dot{J}_q(k_m^{\mathrm{II}}R_b)-\frac{\dot{J}_q(k_m^{\mathrm{II}}R_a)}{\dot{Y}_q(k_m^{\mathrm{II}}R_a)}\dot{Y}_q(k_m^{\mathrm{II}}R_b)}\right], \tag{A.15}$$

where

$$G_{nm}=\sqrt{\frac{h}{h+L}}\epsilon_n\epsilon_m\frac{1}{2}(\mathrm{sinc}((k_{zn}^{\mathrm{I}}+k_{zm}^{\mathrm{II}})h)+\mathrm{sinc}((k_{zn}^{\mathrm{I}}-k_{zm}^{\mathrm{II}})h)). \tag{A.16}$$

Now, recall that the $T$ matrix relates the coefficients $A_{qn}$ and $B_{qn}$ and is defined as

$$B_{qm}=\sum_n(T_q)_{mn}A_{qn}. \tag{A.17}$$

Once the $T$ matrix is known the scattering problem is solved. The $T$ matrix is also used to obtain the effective acoustic parameters of the scatterer [27].

Then, the $T$ matrix can be derived from equations (A.13) and (A.17):

$$(T_q)_{mn}\equiv\sum_k(H_q)_{mk}^{-1}(J_q)_{kn}. \tag{A.18}$$

We are interested here in the single-mode operation, that is, when the mode $n = 0$ in equation (A.2) is the only one excited. This condition implies that the propagating sound does not oscillate in the vertical direction and, consequently, its wavevector is strictly confined in the $XY$-plane. The matrix elements characterizing the equivalent medium are $T_q \equiv (T_q)_{00}$.

It was shown in [27] that the relationship between the $T$ matrix and the $\chi_q$ factor is given, for $q = 0$, by

$$T_0 \approx \frac{\mathrm{i}\pi R_\mathrm{b}^2 k_\mathrm{b}^2}{4} \frac{1 + \frac{1}{2} k_\mathrm{b} R_\mathrm{b} \chi_0}{\frac{k_\mathrm{b}^2 R_\mathrm{b}^2}{2} \ln k_\mathrm{b} R_\mathrm{b} - \frac{1}{2} k_\mathrm{b} R_\mathrm{b} \chi_0}, \tag{A.19}$$

where the term $\frac{k_\mathrm{b}^2 R_\mathrm{b}^2}{2} \ln k_\mathrm{b} R_\mathrm{b}$ in the denominator can, in general, be neglected.

For the case $q = 1$,

$$T_1 \approx \frac{\mathrm{i}\pi R_\mathrm{b}^2}{4} \frac{\chi_1 / k_\mathrm{b} R_\mathrm{b} - 1}{\chi_1 / k_\mathrm{b} R_\mathrm{b} + 1} k_\mathrm{b}^2. \tag{A.20}$$

Note that matrix elements $T_0$ and $T_1$ are obtained from equation (A.18) by calculating the terms given in equations (A.14) and (A.15). Afterwards, the resulting values are inserted into equations (A.19) and (A.20) to extract $\chi_0$ and $\chi_1$. These magnitudes are finally introduced in equations (2*a*) and (2*b*) to calculate $B_\mathrm{a}(\omega)$ and $\rho_\mathrm{a}(\omega)$, respectively.

## References


[1] Fok L, Ambati M and Zhang X 2008 Acoustic metamaterials *MRS Bull.* **33** 931

[2] Torrent D and Sánchez-Dehesa J 2008 Anisotropic mass density by two-dimensional acoustic metamaterials *New J. Phys.* **10** 023004

[3] Torrent D and Sánchez-Dehesa J 2010 Anisotropic mass density by radially periodic fluid structures *Phys. Rev. Lett.* **105** 174301

[4] Zigoneanu L, Popa B I and Cummer S A 2011 Design and measurements of a broadband two-dimensional acoustic metamaterial with anisotropic effective mass density *J. Appl. Phys.* **109** 054906

[5] Spiousas I, Torrent D and Sánchez-Dehesa J 2011 Experimental realization of broadband tunable resonators based on anisotropic metafluids *Appl. Phys. Lett.* **98** 244102

[6] Fang N, Xi D, Xu J, Ambati M, Srituravanich W, Sun C and Zhang X 2006 Ultrasonic metamaterials with negative modulus *Nature Mater.* **5** 452–6

[7] Lee S H, Park C M, Seo Y M, Wang Z G and Kim C K 2009 Double-negative acoustic metamaterials *J. Phys.: Condens. Matter* **21** 175704

[8] García-Chocano V, Graciá-Salgado R, Torrent D, Cervera F and Sánchez-Dehesa J 2012 Quasi two-dimensional acoustic metamaterial with negative bulk modulus *Phys. Rev.* B **85** 184102

[9] Yang Z, Mei J, Yang M, Chan N H and Sheng P 2008 Membrane-type acoustic metamaterial with negative dynamic mass *Phys. Rev. Lett.* **101** 204301

[10] Yao S, Zhou X and Hu G 2010 Investigation of the negative-mass behaviors occurring below a cut-off frequency *New J. Phys.* **12** 103025

[11] Li J and Chan C T 2004 Double-negative acoustic metamaterials *Phys. Rev.* E **70** 055602

[12] Ding Y, Liu Z, Qiu C and Shi J 2007 Metamaterial with simultaneously negative bulk modulus and mass density *Phys. Rev. Lett.* **99** 93904

[13] Cheng Y, Xu J Y and Liu X J 2008 One-dimensional structured ultrasonic metamaterials with simultaneously negative dynamic density and modulus *Phys. Rev.* B **77** 45134

[14] Lee S H, Park C M, Seo Y M, Wang Z G and Kim C K 2010 Composite acoustic medium with simultaneously negative density and modulus *Phys. Rev. Lett.* **104** 054301

[15] Fok L and Zhang X 2011 Negative acoustic index metamaterial *Phys. Rev.* B **83** 214304
[16] Cummer S A and Schurig D 2007 One path to acoustic cloaking *New J. Phys.* **9** 45
[17] Torrent D and Sánchez-Dehesa J 2008 Acoustic cloaking in two dimensions: a feasible approach *New J. Phys.* **10** 063015
[18] Torrent D and Sánchez-Dehesa J 2009 Radial wave crystals: radially periodic structures from anisotropic metamaterials for engineering acoustic or electromagnetic waves *Phys. Rev. Lett.* **103** 64301
[19] Torrent D and Sánchez-Dehesa J 2010 Acoustic resonances in two-dimensional radial sonic crystal shells *New J. Phys.* **12** 073034
[20] Li J, Fok L, Yin X, Bartal G and Zhang X 2009 Experimental demonstration of an acoustic magnifying hyperlens *Nature Mater.* **8** 931
[21] Martin T P, Nicholas M, Orris G J, Cai L W, Torrent D and Sánchez-Dehesa J 2010 Sonic gradient index lens for aqueous applications *Appl. Phys. Lett.* **97** 113503
[22] Climente A, Torrent D and Sánchez-Dehesa J 2010 Sound focusing by gradient index sonic lenses *Appl. Phys. Lett.* **97** 104103
[23] Ambati M, Fang N, Sun C and Zhang X 2007 Surface resonant states and superlensing in acoustic metamaterials *Phys. Rev.* B **75** 195447
[24] Cummer S A, Rahm M and Schurig D 2008 Material parameters and vector scaling in transformation acoustics *New J. Phys.* **10** 115025
[25] Chen H and Chan C T 2010 Acoustic cloaking and transformation acoustics *J. Phys. D: Appl. Phys.* **43** 113001
[26] Park C M, Park J J, Lee S H, Seo Y M, Kim C K and Lee S H 2011 Amplification of acoustic evanescent waves using metamaterials slabs *Phys. Rev. Lett.* **107** 194301
[27] Torrent D and Sánchez-Dehesa J 2011 Multiple scattering formulation of two-dimensional acoustic and electromagnetic metamaterials *New J. Phys.* **13** 093018
[28] Torrent D and Sánchez-Dehesa J 2006 Effective parameters of clusters of cylinders embedded in a nonviscous fluid or gas *Phys. Rev.* B **74** 224305
[29] Torrent D, Håkansson A, Cervera F and Sánchez-Dehesa J 2006 Homogenization of two-dimensional clusters of rigid rods in air *Phys. Rev. Lett.* **96** 204302
[30] Torrent D and Sánchez-Dehesa J 2007 Acoustic metamaterials for new two-dimensional sonic devices *New J. Phys.* **9** 323
[31] Wu Y, Lai Y and Zhang Z Q 2007 Effective medium theory for elastic metamaterials in two dimensions *Phys. Rev.* B **76** 205313
[32] Martin T P, Layman C N, Moore K M and Orris G J 2012 Elastic shells with high-contrast material properties as acoustic metamaterial components *Phys. Rev.* B **85** 161103
[33] Krokhin A A, Arriaga J and Gumen L N 2003 Speed of sound in periodic elastic composites *Phys. Rev. Lett.* **91** 264302